Performance evaluation of an all-optical multicasting strategy based on cross-gain modulation (XGM) in a single semiconductor optical amplifier (SOA)

KARAMDEEP SINGH[a,*], PRABHDEEP KAUR[a], SUNIL KUMAR SINGLA[b], GAGANDEEP KAUR[b]
[a]*Department of Electronics Technology, Guru Nanak Dev University, Amritsar, Punjab, 143005, India*
[b]*Department of Electrical & Instrumentation Engineering, Thapar Institute of Engineering and Technology, Patiala, Punjab, 147001, India*

In this paper, performance of an all-optical multicasting strategy based on harnessing of gain nonlinearity characteristics of semiconductor optical amplifier (SOA) has been evaluated for variety of configurations structured around 4 probe channel spacings. The proposed strategy is very simple as only a single SOA has been deployed in realization purposes. Simulation results in terms of the designated performance metric: Quality factor (Q-factor), demonstrate proposed strategy's capability to multicast an approaching optical signal (3 nm at 40 Gbps, 2 nm at 40 Gbps, 1 nm at 30 Gbps and 0.5 nm at 20 Gbps) onto outgoing signals utilizing XGM property of SOA.

(Received July 24, 2019; accepted February 17, 2020)

Keywords: Nonlinear optics, Cross-gain modulation (XGM), Semiconductor optical amplifier (SOA), All-optical Multicasting, Wavelength conversion

1. Introduction

High-speed large-capacity optical networks require all-optical signal processing to execute data information solely in the optical domain to overcome the issue of optic to electric and vice versa conversions (O-E-O). As an integral technique of most optical signal processing structures, wavelength multicasting technique use different optical carrier wavelengths in networks to transfer combined data to multiple places and have capability to decrease the network resources in contrast with unicast networks [1-3]. Different all-optical multicasting strategies have been developed in past by exploiting several non-linear effects such as four-wave mixing (FWM) [4], cross phase modulation (XPM) [5], nonlinear polarization switching [6], cross gain modulation (XGM) [7] in non-linear platforms such as semiconductor optical amplifier [SOA], highly non-linear fibers (HNLFs) [8] and electro-absorption modulators (EAMs) [9] etc. All the strategies mentioned previously have their specific advantages and drawbacks in terms of several operational characteristics such as operating wavelength range, production cost, and system complexity [4-9].

Specifically, it has been observed that SOA seems most suitable candidate for design of all-optical multicasting strategy due to its several attractive features such as wide wavelength range, low cost, higher conversion efficiency, insensitivity to the polarization of input signals and high non-linearity [10].

A few XGM in SOA based multicasting techniques have been reported so far, for instance, Contestabile et al. 2006 [7] proposed a double stage XGM in SOA based technique for 1-to-8 channels multicasting capable of operating at 10 Gbps. Lee et al. 2006 [11] presented an all optical multicasting strategy utilizing dual stage XGM in SOA for 16 channels at 10 Gbps. Contestabile et al. 2011 [12] demonstrated all optical wavelength multicasting using QD-SOA for 1 to 4 channels at 40 Gbps. Hui et al. 2014 [13] presented multicasting technique using XPM in DHNPCF at 20 Gbps for eight channels. Further, Hui et al. 2015 [14] also described another technique by using XPM in DHNPCF for 4 channels at 10 Gbps. Bao et al. 2016 [15] proposed multicasting scheme by using Kerr effect in PPLN waveguide.

It has been observed from the study of open literature available that all techniques based on XGM harnessing in SOAs are restricted to maximum of 1-to-16 channels and further, the maximum bit rate of operation reported is ≤ 40 Gbps. But, in future, much improved all-optical multicasting strategies are required, which can efficiently multicast more number of channels and at much higher bit rate of operations.

The novelty of proposed work is capability of much more number of channels (> 16) using only a single SOA as compared to earlier reported implementations [7-15].

In this article, we have simulated and evaluated the performance of XGM in SOA based wavelength multicasting strategy which is capable of multicasting a number of channels, simultaneously and operating up to 40 Gbps rate. The proposed XGM in SOA multicasting strategy has been simulated for several simultaneous channels which are spaced at a) 3 nm, b) 2 nm, c) 1 nm and d) 0.5 nm from each other. In proposed strategy, all-optical multicasting has been realized by injecting one pump signal and multiple probe signals centered at multiple wavelengths around pump signals inside a single

SOA.

Rest of the article is organized as follows: Section 2, illustrates the concept of proposed multicasting technique. In Section 3, system setup used for demonstration purposes along with all system parameters is presented. Section 4 is related with results and discussions. Conclusions are addressed in section 5.

2. System setup

The operational principle of proposed all-optical multicasting strategy based on XGM exploitation in a single SOA is depicted in Fig. 1.

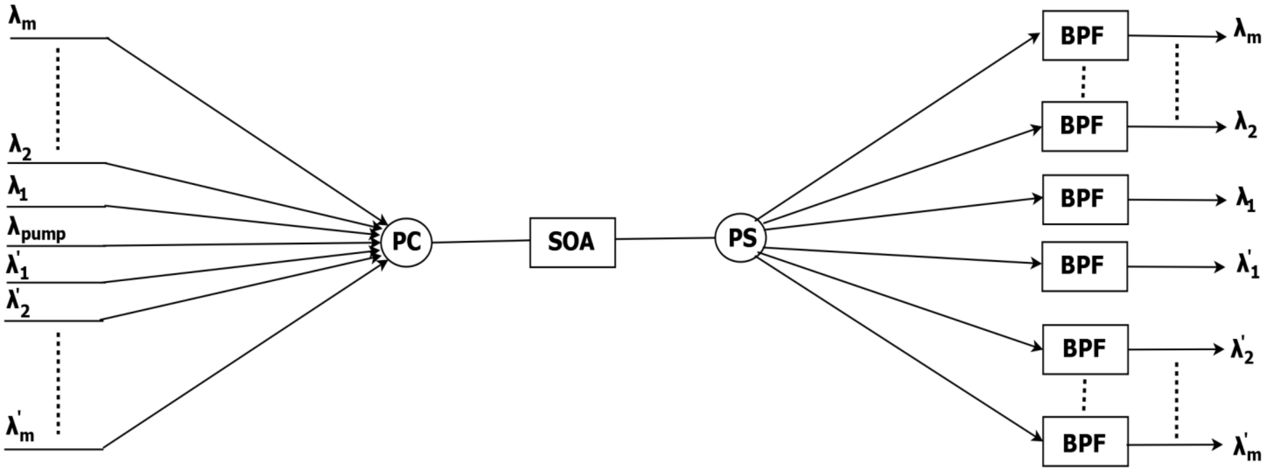

Fig. 1. Operational principle of the all-optical multicasting using XGM in SOA

As shown in Fig. 1, multiple probe signals centered at respective wavelengths $(\lambda_1, \lambda_2, \dots, \lambda_m, \lambda_1', \lambda_2', \dots, \lambda_m')$ are injected inside a single SOA along with a pump signal centered at λ_{pump}. With the help of power combiner (PC). In order to implement multicasting, XGM in SOA has been exploited in order to execute wavelength conversion operation. The gains of the probe signals differ inversely with the power of the pump signal by keeping the saturation point. Data of the pump signal is inversely imposed on all probe signals travelling alongside it in a single SOA [11]. It happens because of occurrence of XGM process in SOA, that allows this single SOA structure to copy an individual highly intense input signal (pump signal) onto the low energy probe signals centered at multiple neighboring wavelengths $(\lambda_1, \lambda_2, \dots, \lambda_m, \lambda_1', \lambda_2', \dots, \lambda_m')$ [11]. The formula for small dynamic gain variation Δg (t_1, z_1) around gain g (t, z) because of XGM between multiple channels inserted in gain recovery optimized SOA is [16-17]:

$$\Delta g\left(t_{1,}z_1\right) = \left[\frac{A_g\Gamma}{\tau_e P_L}\left[\frac{I\tau_e}{wqt} exp\left(\frac{\Delta P_1}{\tau_e}\right) + \sum_{n=1}^{M}\frac{(-1)^n}{P_L^{n-1}} exp\left(\frac{\Delta \mathrm{P_n}}{\tau_\mathrm{e}}\right) \times L\left[\overline{N}(t_n, z_n) - (N(t,z) - N_0)\overline{P^{n-1}}(t_{n-1}, z_{n-1})\right]\right]\right] \quad (1)$$

where, $\Delta \mathrm{P} = \mathrm{P}(t_2, z_2) - \mathrm{P}(t_1, z_1)$ & $\mathrm{N}(t_n, z_n)$ symbols represent time variation of power and carrier density, respectively, whereas, derivative power coefficient and derivative carrier density are $P_L = \frac{\partial \mathrm{P}(t_1, z_1)}{\partial t_1}$ and $\overline{N} = \frac{\partial \mathrm{N}(t_1, z_1)}{\partial t_1}$, respectively. Where L in amplifier length, I is the injection current, N (t , z) is the injected carrier density, w & t are active region width & thickness, respectively and q is charge on electron. Further, N_0 is the carrier density at transparency and A_g is differential gain coefficient, Γ is optical confinement factor and the effective carrier lifetime is represented by symbol τ_e [16-17]. Then, these probe signals are separated using are passed through respective butter-worth band pass filters (BPF) which are centered at appropriate wavelengths after passing through power splitter (PS).

3. System setup

System setup utilized for the demonstration of proposed all-optical wavelength multicasting strategy is shown in Fig. 2.

As shown in Fig. 2, a pseudo-random binary sequence (PRBS) generator has been utilized to produce random data. Logical data obtained from PRBS generator are then converted into electrical Gaussian pulses of duty cycle (50%) by utilizing a RZ pulse driver. One continuous wave (CW) laser centered at 1550 nm has been utilized as optical carrier signal. The optical carrier signal generated by CW laser launched into mach-zehnder modulator (MZM). The optical modulated data stream generated by MZM is further put into an optical amplifier (erbium doped fiber amplifier) which amplifies the optical data. Other tunable CW lasers, which are centered at 1549.5 nm, 1549.0 nm, 1550.5 nm, 1551.0 nm etc. are 0.5 nm spaced apart, are further utilized to generate probe signal at different wavelengths for multicasting purposes. The pump signal which carrying data @1550.0 nm and other probe signals (1549.5 nm, 1549.0 nm, 1550.5 nm, 1551.0 nm etc.) are then combined together by utilizing a power combiner (PC) and injected into a single gain recovery time optimized SOA [16-17] as illustrated in Fig. 2. The SOA physical and operational parameter values used in this study are elucidated in Table 1.

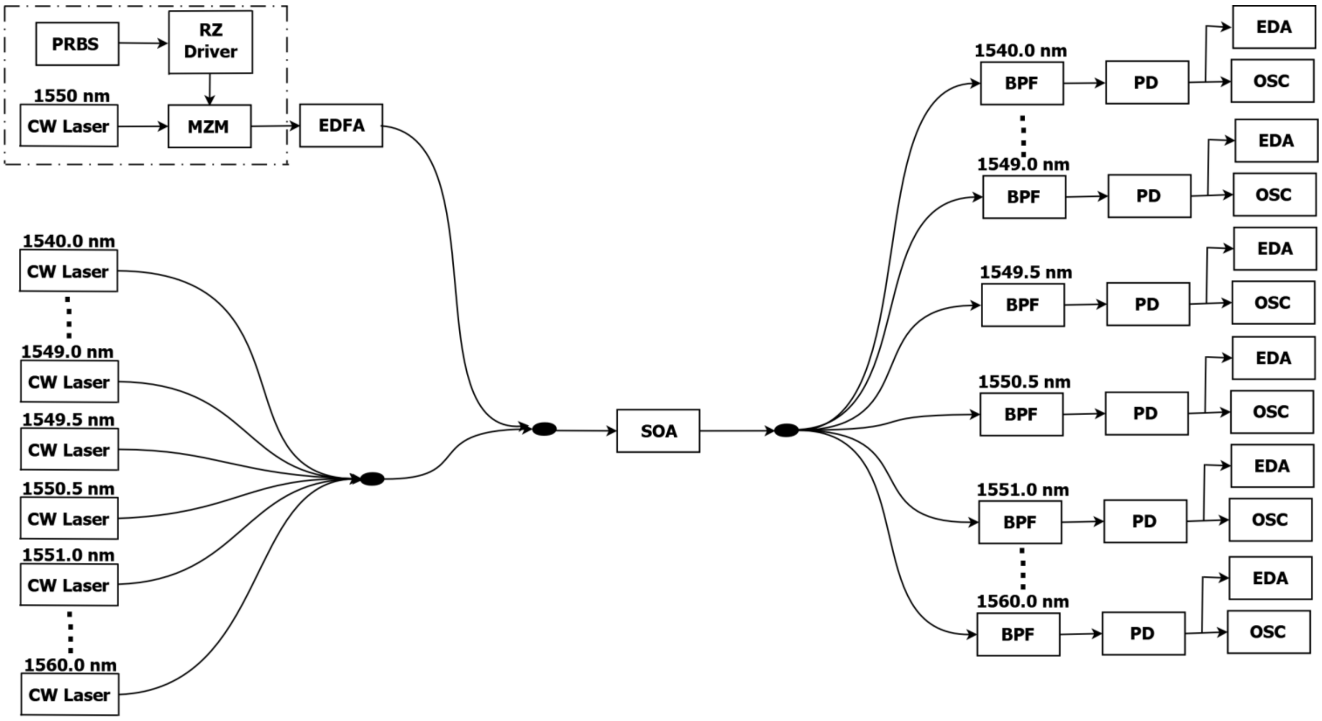

Fig. 2. System setup of proposed all-optical wavelength multicasting strategy

Table 1. SOA physical parameters [16-17]

Sr. No.	SOA parameter	Value
1.	Injection current (*I*)	600 mA
2.	Amplifier length (*L*)	300 µm
3.	Active region width (*w*)	1 µm
4.	Active region thickness (*t*)	0.1 µm
5.	Optical confinement factor (Γ)	0.4
6.	Differential gain (A_g)	2.78×10^{-20} m^2
7.	Transparency carrier density (N_0)	1.4×10^{24} m^3
8.	Linear recombination coefficient (A_{nr})	1.43×10^{8} s^{-1}
9.	Bimolecular recombination coefficient (B_{sp})	1×10^{-16} m^3 s^{-1}
10.	Auger recombination coefficient (C_a)	3×10^{-41} m^6 s^{-1}
11.	Initial carrier density (*N*)	3×10^{24} m^{-3}

As shown in Fig. 2, when number of low powered probe signals (1549.5 nm, 1549.0 nm, 1550.5 nm, 1551.0 nm etc.) are injected along with a high-powered pump signal (1550.0 nm) inside a single gain recovery optimized SOA, the XGM is bound to be occurred on low power probe signals. Due to occurrence of XGM effect in a single SOA, the variations of modulated pump signal are imprinted on different probe wavelengths injected alongside it, thus in turn attainment of all-optical multicasting for different probe channels spacings (0.5 nm, 1 nm, 2 nm, 3 nm). Further, the XGM impacted probe signals are extracted by using band pass optical filters (BPF) centered at respective wavelengths. These extracted XGM impacted probe signals are then fed into respective receiver sections. For signal analysis purposes, an oscilloscope (OSC) and an eye diagram analyzer (EDA) has been used in all receiver sections as shown in Fig. 2.

4. Results and discussions

The operation of proposed all-optical wavelength multicasting technique based on XGM SOA has been verified by injecting 16-bit long random input patterns produced by PRBS generators at 10 Gbps, 20 Gbps, 30 Gbps and 40 Gbps bit rates and then performing bit-by-bit checking of results generated for different probe spacing (3 nm, 2 nm, 1 nm and 0.5 nm) as shown in Fig. 3-4.

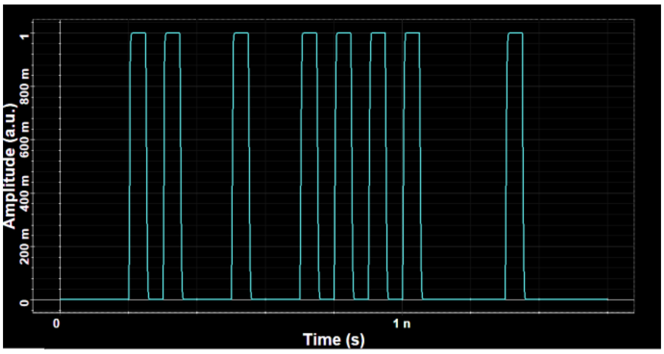

Fig. 3. Temporal trace for input signal at 10 Gbps

An example of operation of proposed strategy in terms of recorded output bit sequence for different probe channel spacing's (0.5 nm, 1 nm, 2 nm & 3 nm) at 40 Gbps line rate is depicted in Fig. 4 (a-d). It can be clearly observed from Fig. 4 (a-d) that for different probe wavelength spacing configurations, the proposed XGM in a single SOA based multicasting strategy, results in generation of correct bit pattern (1100101000011011) which is inverted version of input signal at 40 Gbps.

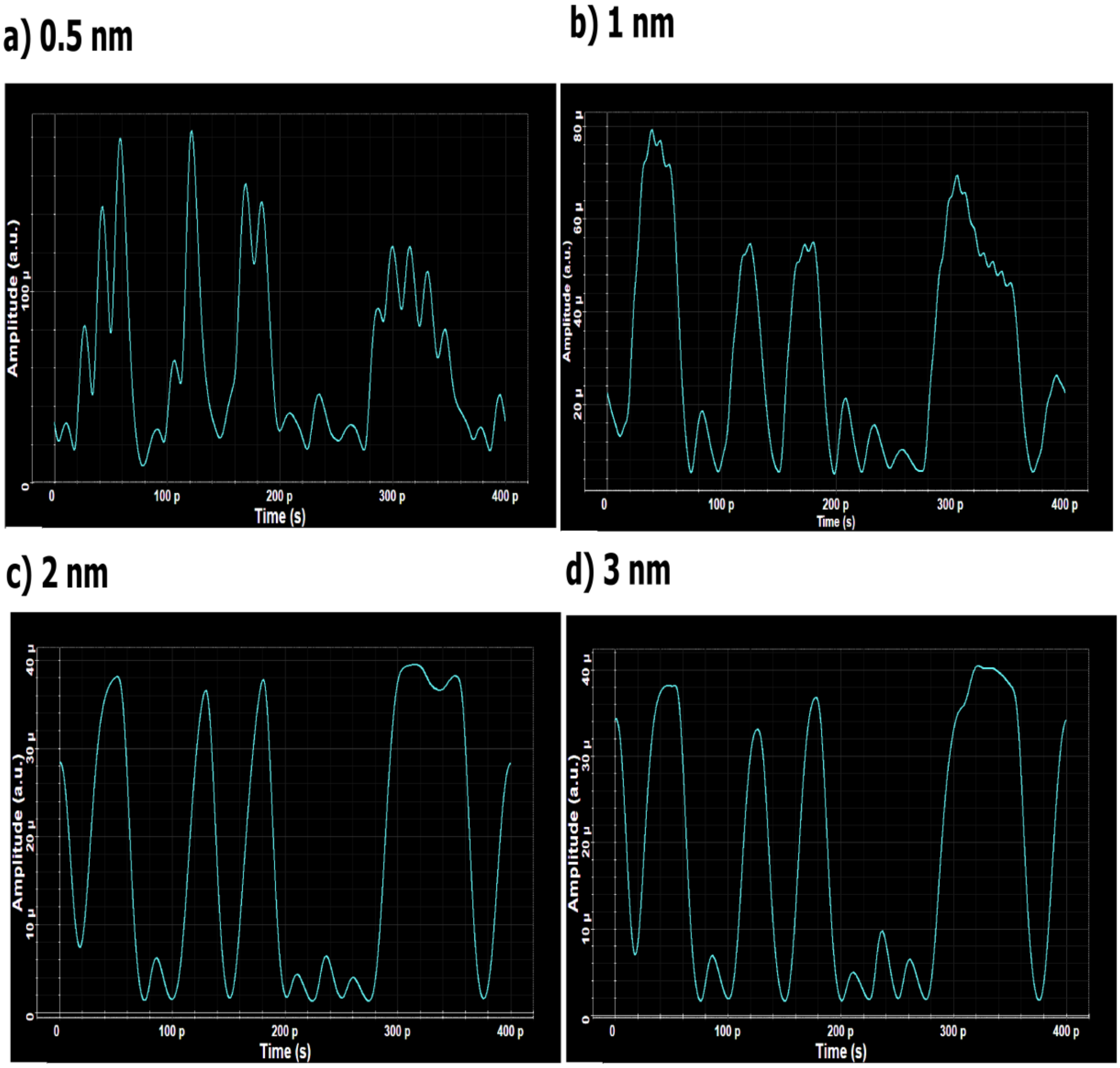

Fig. 4. Temporal traces for multicast output probe signals spaced at a) 0.5 nm spacing, b) 1 nm spacing, c) 2 nm spacing, d) 3 nm spacing at 40 Gbps line rate

It has been noticed that proposed XGM based multicasting strategy exhibits best results when probe channels are spaced at 3 nm while performance begins to degrade as spacing between probe signals is decremented i.e. from 3 nm to 2 nm, 2 nm to 1 nm and 1 nm or 0.5 nm as seen in Fig. 4 (a-d). The prominent factor that results in degradation of performance of proposed all-optical multicast strategy is occurrence of another non-linear effect found in SOAs, which takes place due to decrease in probe channel spacing. This non-linear effect is called four-wave mixing (FWM) effect. The by-products of the FWM effect, meddle with the original probe signal wavelengths, and can originate intra-band crosstalk as shown in Fig. 4 (a-d).

Furthermore, as we increment the operating bit rate, performance degradation happens. The degradation in performance is due to the fact that when operating bit rate is increased, SOA don't get enough time to recover their gain, so ultimately performance degrades. In order to illustrate this degradation in performance of proposed multicasting strategy when bit rate is incremented, eye diagrams of the one of output multicast signal (1511 nm) have been calculated by considering 256 bits long input random sequences for different probe spacing strategies (3 nm, 2 nm, 1 nm & 0.5 nm) at different bit rates (10, 20, 30 and 40 Gbps) and are presented in Fig. 5 (a-d) as follows.

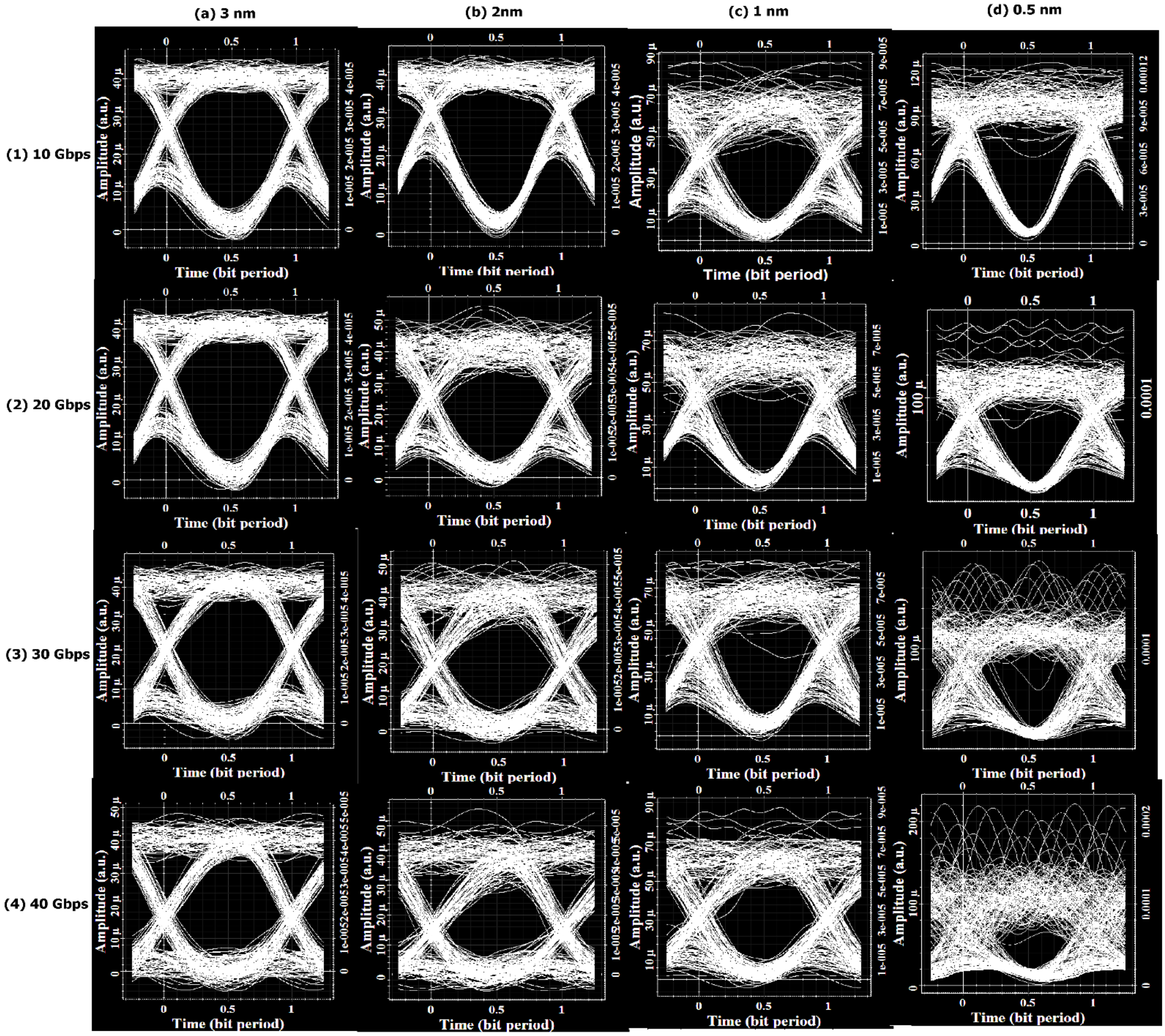

Fig. 5. Calculated eye diagrams for multicast output at a) 10 Gbps, b) 20 Gbps, c) 30 Gbps, d) 40 Gbps for different probe spacings (3 nm, 2 nm, 1 nm & 0.5 nm)

It could be seen that clear and open eye diagrams have been achieved for every single output for 3 nm & 2 nm cases up to 40 Gbps as depicted in Fig. 5 (a-d), which indicates successful realization of all-optical multicasting technique utilizing XGM effect in a single gain recovery optimized SOA. However, as the channel spacing between probe signals is decreased from 3 nm to 0.5 nm level, degraded performance can be clearly seen, which is credited to occurrence of FWM effect. Furthermore, as operating bit rate is increased beyond 20 Gbps level, because of limited gain recovery time of SOA employed, overall performance is degraded. Moreover, in order to quantify the quality of realized multicasting outputs, Quality-factor (Q-factor) has been measured, which is defined as follows [16-17]:

$$Q = \frac{P^1 - P^0}{\sigma^1 + \sigma^0} \tag{2}$$

where, P^0 symbol represents low state (0-state) and P^1 symbol represents high state (1-state) average output powers whereas, σ^0 and σ^1 signs indicate standard deviations of low state (0-state) and high state (1-state), respectively [16-17]. The Q-factor variations obtained of all-optically XGM in SOA based multi-casted outputs for 4 different probe channel spacing's (3 nm, 2 nm, 1 nm & 0.5 nm) at different operating bit rates are depicted in Fig. 6 (a-d).

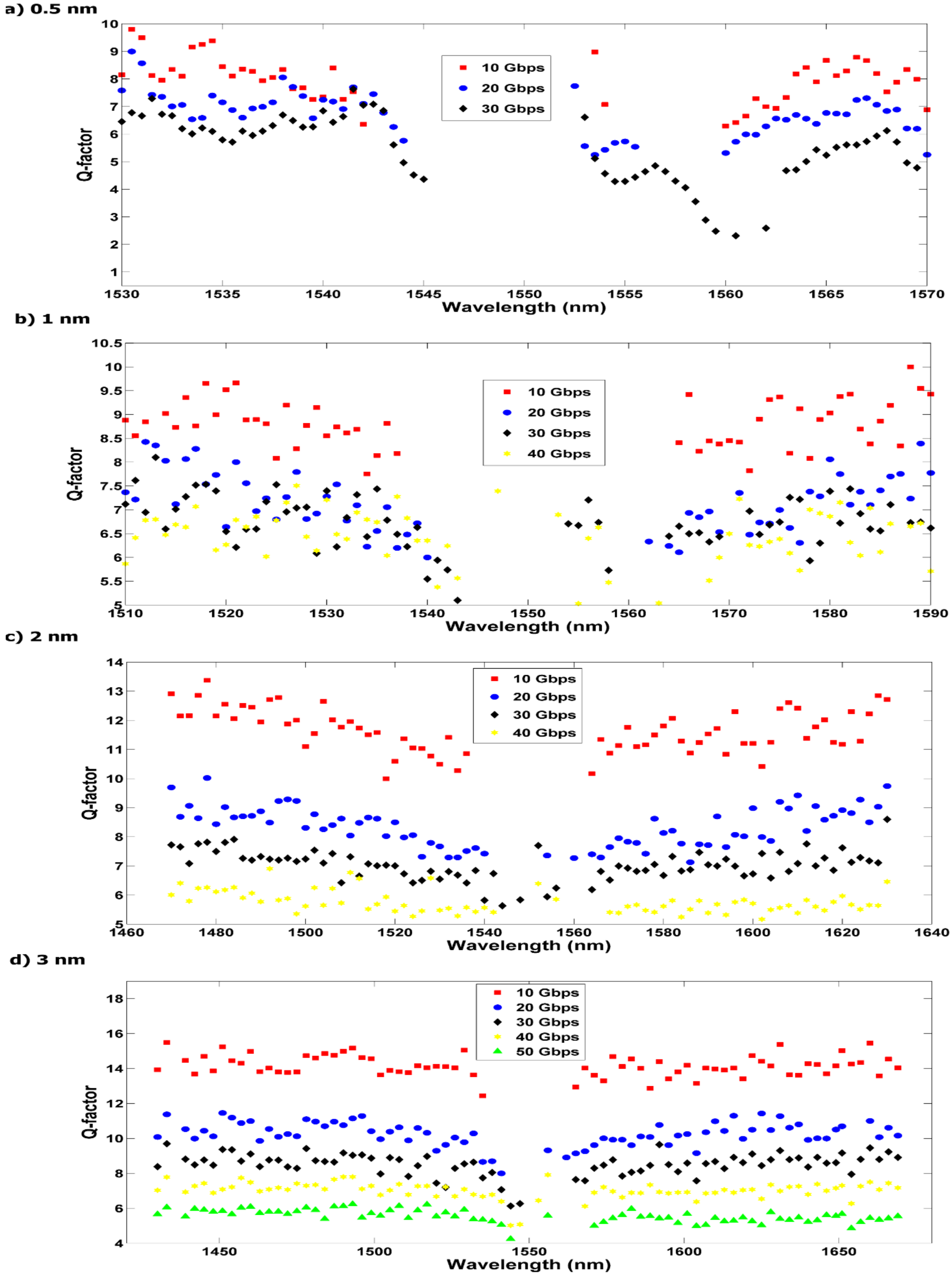

Fig. 6. Quality-factor versus wavelength (nm) for various probe spacings a) 0.5 nm, b) 1 nm, c) 2 nm & d) 3 nm at various operating data rates (Gbps) (color online)

The observation of Fig. 6 (a-d) consolidates the earlier said fact that as bit rate of operation is incremented, the performance of proposed XGM in SOA based strategy decreases. This degradation occurs because SOA does not get enough time to recover its gain. Further, it can be noticed in all probe spacing cases i.e. 3 nm, 2 nm, 1 nm & 0.5 nm, that performance of probe channels which are adjacent to pump signal is comparatively degraded. Such behavior can be credited to occurrence of dominant spurious FWM products around center frequency pump signal which is 1550 nm in present case. It can be observed from Fig. 7 (a) that XGM in SOA based all-optical multicasting strategy for 0.5 nm spaced probe signals can operate up to maximum rate of 30 Gbps. Whereas, other all-optical multicasting strategy for 1 nm, 2 nm and 3 nm spaced probe signals can operate up to maximum rate of 40 Gbps, 40 Gbps and 50 Gbps, respectively.

Further, in order to illustrate, the level of development achieved using the proposed XGM in a single SOA based multicasting technique, a comparison with earlier reported multicasting techniques is presented in Table 2.

Table 2. Comparison of proposed XGM in a single SOA based multicasting strategy with earlier reported multicasting strategies

Author Name and year	Parameters			
	Non-linear phenomena	Number of non-linear mediums	No. of channels	Operating bit rate
Contestabile et al. (2006) [7]	XGM	2 SOAs	8	10 Gbps
Lee et al. (2006) [11]	XGM	2 SOAs	16	10 Gbps
Contestabile et al. (2011) [12]	FWM	1 Quantum - Dot Semiconductor Optical Amplifier (QD-SOA)	4	40 Gbps
Hui (2014) [13]	XPM	1 Dispersion Flattened Highly Nonlinear Photonic Crystal Fiber (DHNLPCF)	8	20 Gbps
Hui et al. (2015) [14]	XPM	DHNLPCF	4	10 Gbps
Bao et al. (2016) [15]	Kerr-Effect	1 PPLN	7	20 Gbps
Present work	XGM	1 SOA	80	30 Gbps

It can be observed from Table 2, that proposed XGM in single SOA based multicasting strategy is better as compared to some earlier reported strategies as:

- As only a single SOA has been used for realization purposes, which is a considerable advantage over schemes proposed by Contestabile et al. (2006) [7] & Lee et al. (2006) [11].
- The proposed XGM in single SOA based multicasting strategy also outperforms some of earlier reported multicasting strategies purposed by Contestabile et al. (2006) [7], Lee et al. (2006) [11], Hui (2014) [13], Hui et al. (2015) [14] and Bao et al. (2016) [15] in terms of bit rate of operation.

5. Conclusions

We have exhibited and evaluated performance of all-optical multicasting strategy based on XGM in a single gain recovery optimized SOA for different probe channel spacings (3 nm, 2 nm, 1 nm & 0.5 nm) at various bit rates. It has been shown by carrying out numerical simulations that proposed strategy is compatible for multicasting several simultaneous channels, all-optically. Simulation results obtained in terms of Q-factor indicate the successful execution as Q-factors > 6 have been recorded for each multicast output signal in every probe spacing configuration. The proposed XGM in a single gain recovery optimized SOA based all-optical multicasting technique can operate for following maximum operating rates: A) 0.5 nm: 20 Gbps, B) 1 nm: 30 Gbps, C) 2 nm: 40 Gbps, D) 3 nm: 40 Gbps.

References

[1] K. Singh, G. Kaur, M. L. Singh, Opt. Quantum Electron. **48**(9), 418 (2016).
[2] K. Singh, G. Kaur, M. L. Singh, Opt. Fiber Technol. **24**, 56 (2015).
[3] K. Singh, G. Kaur, M. L. Singh, Opt. Eng. **55**(7), 077104 (2015).
[4] G. Contestabile, M. Presi, E. Ciaramella, IEEE Photon. Technol. Lett. **16**(7), 1775 (2004).
[5] L. Rau, B. E. Olsson, D. J. Blumenthal, In Optical Fiber Communication Conference 2001 (p. WDD52).
[6] G. Contestabile, N. Calabretta, M. Presi, E. Ciaramella, IEEE Photon. Technol. Lett. **17**(12), 2652 (2005).
[7] G. Contestabile, N. Calabretta, R. Proietti, E. Ciaramella, IEEE Photon. Technol. Lett. **18**(1), 181 (2006).
[8] J. Wang, Q. Sun, J. Sun, X. Zhang, Opt. Commun. **282**(13), 2615 (2009).
[9] K. K. Chow, C. Shu, Electron. Lett. **39**(19), 1395 (2003).
[10] M. Matsuura, N. Kishi, T. Miki, In European Conference on Optical Communications, ECOC 2006. (pp. 1-2).
[11] B. H. Lee, R. Mohamad, K. Dimyati, IEEE Photon. Technol. Lett. **18**(21), 2215 (2006).
[12] G. Contestabile, A. Maruta, S. Sekiguchi, K. Morito, M. Sugawara, K. I. Kitayama, IEEE J. Quantum Electron. **47**(4), 541 (2011).
[13] Z. Q. Hui, Sci. World J. Vol. 2014, pp. 1-9 **(**2014).
[14] Z. Q. Hui, B. Zhang, J. G. Zhang, J. Mod. Opt. **63**(8), 724 (2016).
[15] C. Bao, P. Liao, A. Kordts, M. Karpov, M. H. Pfeiffer, L. Zhang, Y. Yan, G. Xie, Y. Cao, A. Almaiman, M. Ziyadi, Opt. Lett. **41**(16), 3876 (2016).
[16] K. Singh, G. Kaur, M. L. Singh, Optoelectron. Adv. Mat. **11**(3-4), 189 (2017).
[17] K. Singh, G. Kaur, M. L. Singh, Photon. Netw. Commun. **34**(1), 111 (2017).

*Corresponding author: karamdeep1989@gmail.com